



Original Research

Evolutionary analysis of TSP-1 gene in Plateau zokor (*MyospalaxBaileyi*) and its expression pattern under hypoxia

Suhua Li^{1,2,4}, Bo Xu³, Zhifang An², Zhijie Wang³, Yongxiao Li³, Lian Wei³, DengbangWei^{1,3*}

¹ State Key Laboratory of Plateau Ecology and Agriculture, Qinghai University, 251 Ningda Road, Xining, Qinghai 810016, China

² Research Center for High Altitude Medicine, Qinghai University, 251 Ningda Road, Xining, Qinghai 810016, China

³ College of Eco-Environmental Engineering, Qinghai University, 251 Ningda Road, Xining, Qinghai 810016, China

⁴ Department of Gastroenterology, Qinghai University Affiliated Hospital, 29 Tongren Road, Xining, Qinghai 810001, China

Correspondence to: weidengbang@163.com

Received November 23, 2018; Accepted March 21, 2019; Published March 31, 2019

Doi: <http://dx.doi.org/10.14715/cmb/2019.65.3.7>

Copyright: © 2019 by the C.M.B. Association. All rights reserved.

Abstract: The plateau zokor (*Myospalaxbaileyi*) is a specialized subterranean rodent that lives on the Qinghai-Tibet Plateau, and has successfully adapted to hypoxic environment. Raised expression of vascular endothelial growth factor (VEGF) and enhanced microvessel density (MVD) in tissues enable subterranean rodents to adapt to hypoxic sealed burrows. However, the expression of VEGF is inhibited by decreases in oxygen content, which is different from what obtains in Sprague Dawley (SD) rats. Thrombospondin-1 (TSP-1) is the first endogenous angiogenesis inhibitor identified in *p53* pathway. It has several domains that bind to different proteins which regulate cell-to-cell interactions, inhibit endothelial cell proliferation and induce endothelial cell apoptosis (anti-angiogenesis). In this study, we analyzed the coding region and the expression pattern of TSP-1 gene in plateau zokor under different oxygen partial pressures using bioinformatics and qRT-PCR, respectively. Our results showed that the base and amino acid homologies between plateau zokor and Northern Israeli blind subterranean mole rat (*Nannospalaxgalili*) were 95.08 and 97.61%, respectively. There were eight parallel evolution sites with *Nannospalaxgalili*. Evaluation by 'Sorting Tolerant From Intolerant' (SIFT) algorithm showed four sites with significant effects on the function of TSP-1. Three-dimensional (3D) structures revealed that Asp185 and Thr270 were located in the NH₂ terminal domain, with Glu536 in the Type I repeat domain, and Thr1092 in the COOH terminal domain. Compared to SD rats, the polarities of these four mutation sites changed. The expression levels of TSP-1 in plateau zokor tissues increased significantly from 2 260 m (16.12kPa) to 3 300 m (14.13kPa), but there was no significant difference in TSP-1 expression in SD rats. In conclusion, due to long-term adaptation to the hypoxic environment of sealed burrows, plateau zokor upregulates the expression of TSP-1 to effect anti-angiogenesis. Moreover, mutations in gene structure of TSP-1 may play an important role in inhibiting angiogenesis.

Key words: Plateau zokor (*Myospalaxbaileyi*); Evolutionary analysis; TSP-1; Hypoxia.

Introduction

Angiogenesis is the physiological process by which new blood vessel capillaries are formed, and it is tightly regulated by a balance between pro-angiogenic and anti-angiogenic factors (1). Under hypoxic conditions, the levels of hypoxia-induced factor-1 α (HIF-1 α) are stabilized. With reduction in oxygen content, the ability to activate the transcription of VEGF by binding with hypoxia response element (HRE) is enhanced (2, 3). Meanwhile, HIF-1 α combines with *p53* to enhance the transcription of downstream anti-angiogenesis factors, resulting in inhibition of unlimited growth of microvessels in hypoxic environment (4). These factors are TSP-1, angiostatin and platelet factor-4(5,6).

Thrombospondin-1 (TSP-1) is a disulfide-bonded trimer with several different domains: NH₂-terminal domain, procollagen homology domain (PC¹), type I (thrombospondin structural or properdin-like) repeats, type II (EGF-like) repeats, type III (calcium-binding) repeats, and COOH-terminal domain (7). These bind to low density lipoprotein receptor-like protein (LRP1), CD36 and integrin-associated protein CD47(IAP) to

inhibit angiogenesis and metastasis by regulating cell-to-cell interaction and proliferation of endothelial cells, and induce endothelial cell apoptosis (8, 9). Studies have demonstrated that amino acid mutations in TSP-1 type I repeat domain in patients with pulmonary hypertension activated TGF-beta and CD36, and increased the proliferation rates of endothelial cells and smooth muscle cells, suggesting that structural mutations have impact on function (10). The expression level of TSP-1 is low under normal conditions, but it increases gradually with decrease in oxygen content, and is negatively correlated with micro-vessel density (MVD). Thus, hypoxia inhibits the growth of microvessels by upregulating the expression of TSP-1 (11-14).

The plateau zokor (*Myospalax baileyi*) is small native mammal distributed in the Qinghai-Tibetan Plateau from 2000 m to 4200 m. They spend their whole life cycle in sealed burrows which are characterized by remarkable hypoxia and high carbon dioxide levels. At an altitude of 3200 m, the average oxygen concentration is 156.68 g/m³ in the borrows of plateau zokor (15). Currently, the most extensive research on subterranean rodent is on the family of Spalaxidae which comprises

Myospalacinae, Spalacidae and Rhizomyinae subfamilies called “mole rats” (16). *Nannospalax galili* belongs to the subfamily of Spalacidae which lives in the upper Galilee mountains in northern Israel at an altitude about 600m (oxygen content in the atmosphere is about 19.76%) and belongs to the *Spalax ehrenbergi* superspecies (17, 18). However, studies have found that the plateau zokor has *in vivo* normoxia at such hypoxic environments, suggesting that after long-term evolution and natural selection like other subterranean rodents, they have produced a series of phenotypic, physiological and genomic strategies to adapt to their harsh environment. They have smaller area of pulmonary alveolar and bigger volume of lungs which enhance oxygen uptake. They have increased counts of red blood corpuscle and contents of myoglobin and hemoglobin which facilitate transport of oxygen (19-24). Abundance of capillaries in the alveolar septum and mitochondria in muscle cells increase blood flow to the lungs and the surface area for gas exchange, and reduce barrier to oxygen consumption (25, 26). These strategies explain their distinguished ability at adaptation (27). Transcriptome studies have revealed that under hypoxic environments, positive selection and convergence evolution sites occur in some genes of the plateau zokor (28). The micro-vessel density (MVD) of plateau zokor in hypoxic environment is significantly higher than that of the SD rat. This enhances the transport of O₂, nutrients and metabolites, and is an important mechanism used by the plateau zokor to adapt to hypoxia (29). It has been shown that in *Spalax*, the MVD increased 2-fold, but the expression level of VEGF decreased 2-fold, relative to SD rat, in the brain and skeletal muscle kept at 6% O₂ for 4 h (30). In *Myospalax baileyi*, the MVD in the liver and brain were significantly increased, relative to SD rat at an altitude of 3200 m, compared to an altitude of 2300 m. Interestingly, the VEGF expression level significantly decreased in *Myospalax baileyi* (20). These findings indicate that the expression pattern of angiogenesis in subterranean rodent is different from that in SD rat under hypoxia, due to upregulated expressions of angiogenic growth inhibitors.

The sequence characteristics of TSP-1 and the response to hypoxia in *Myospalax baileyi* are not well understood. Therefore, in the present study, we used bioinformatics analysis of the evolution of TSP-1 in plateau zokor to investigate whether there existed similarities with, and differences from other subterranean species. In addition, differences in TSP-1 expression between low and high altitudes in plateau zokor tissues using qRT-PCR were investigated.

Materials and Methods

Sample collection and treatment

Plateau zokors were trapped alive at Zongjiagou region in Huangyuan County, Qinghai Province, China. They were divided into two groups: (1) high altitude group zokors captured at an altitude of 3300m where the oxygen partial pressure and oxygen content were 14.13kPa and 193.4 g/m³, respectively; and (2) low altitude group zokors captured in the Zongjiagou region and raised for 8 days in Xining City, Qinghai Province, China at an altitude of 2260m at oxygen partial pressure

and oxygen content of 16.12kPa and 229.7 g/m³, respectively. Sprague Dawley (SD) rats were bought from Lanzhou City, Gansu Province, China. The rats were divided into two groups: (1) high altitude group rats raised in the Zongjiagou region at an altitude of 3300m for 8 days; and (2) low altitude group of rats raised in Xining City, Qinghai Province, China at an altitude of 2260m for 8 days. The sample size was 8 animals per group. All animals were anaesthetized with sodium pentobarbital (5%) and sacrificed using cervical dislocation immediately before dissection. Liver, lung and skeletal muscles tissues of plateau zokor were rapidly removed and quickly frozen in liquid nitrogen. The RNA extraction, cDNA library construction and the next generation sequencing (NGS), and Isoform Sequencing (Iso-Seq) library construction were performed according to the procedure of Novogene Bioinformatics Technology Co. Ltd, Beijing, China. The NGS and Iso-Seq were sequenced on Illumina HiSeq 4000 and PacBio RSII platform, respectively. All procedures involved in the handling and care of animals were in accordance with the China Practice for the Care and Use of Laboratory Animals. The study was approved by the China Zoological Society (permit number: GB 14923-2010).

TSP-1 CDS sequence acquisition

Trinity fasta format gene in the NGS transcriptional databases and the flnc gene in the Iso-Seq Transcriptional databases were used to build local databases using ncbi-blast- 2.7.1 program (<https://ftp.ncbi.nlm.nih.gov/blast/executables/LATEST>). Complete TSP-1 coding sequences of *Nannospalax galili* were used as query sequences to find the homologous sequences or fragments by local blast. The fragments were resembled and translated using Lesergene 7.0 program (31). All selected sequences were used to construct a homologous tree using MEGA7.0 program. The sequence with the highest homology with *Nannospalax galili* was selected as the coding sequence of target protein. Then, the sequence was screened by DNAMAN version 9.0 (<http://www.lynnon.com>) from three Iso-Seq Transcriptional databases and one PacBio Transcriptional database, and the final Plateau zokor TSP-1 sequence was selected. Complete TSP-1 coding sequences for 23 mammalian species (including 13 Rodentia, 4 Lagomorpha and 6 other mammalian species serving as Outgroup) were downloaded from 23 available published mammalian genome sequences from National Center for Biotechnology Information (NCBI; www.ncbi.nlm.nih.gov).

Prediction of physicochemical properties and homology comparison

The physicochemical properties of TSP-1 amino acid sequences of *Myospalaxbaileyi*, *Nannospalaxgalili* and *Rattus norvegicus* were predicted using the ProtParam tool (<http://web.expasy.org/protparam/>). Nucleotide sequences of each TSP-1 and their deduced amino acid sequences were aligned separately using ClustalW2 (<http://www.ebi.ac.uk/Tools/msa/clustalw2>) and MEGA 7.0(32). The maximal likelihood tree based on TSP-1 coding sequences and amino acid sequences of 24 species were constructed using MEGA 7.0.

Construction of tree species from mitochondrial DNA data

We use mitochondrial DNA sequences to construct phylogenetic tree in order to reflect the relationship among species more scientifically, and to prepared for the next selective pressure analysis and evolutionary analysis. The complete mitochondrial DNA (mtDNA) sequences for 24 mammalian species were downloaded from NCBI (www.ncbi.nlm.nih.gov), including fourteen rodents, four lagomorphas, four artiodactylas and two primates. The mtDNA phylogenetic trees were reconstructed using MrBayes 3.2.6 (33). Bayesian inference (BI) with Markov-chain Monte Carlo (MCMC) (34) sampling was performed using MrBayes 3.2.6 run for one million generations. Two simultaneous runs were made, sampling trees every 1,000 generations, with three heated and one cold chain to encourage swapping among the MCMC chains and to avoid the analysis remaining in local rather than global optima. ModelTest (35) was used to select the optimal models based on the Akaike Information Criterion (AIC) (36-38). Convergence of sampled parameters and potential autocorrelation (effective sampling size/ESS for all parameters >200) were investigated in Tracer 1.6 (<http://tree.bio.ed.ac.uk/software/tracer/>). Moreover, the average SD of split frequencies between both runs was checked (<0.01). The Bayesian posterior probabilities were obtained from the 50% majority rule consensus of the post-burn-in trees sampled at stationarity, after removing the first 25% of trees as a “burn-in” stage.

Selection pressure analyses

The sequence alignment was obtained using ClustalX1.81 and format conversion was performed with MEGA7.0 software. The maximum-likelihood method was used to estimate the positive sites using branch-site models in codeml from the PAML4.8 software package (39) based on the 24 mammalian species tree. Positive selection was detected using branch-site model A, in which ω varies among sites along specific lineages (40). The significance of the likelihood ratio test (LRT) statistic was determined by Chi-squared test (41).

Selective pressure was tested based on the phylogeny by comparing the non-synonymous/synonymous substitution ratios ($\omega = dN/dS$) with $\omega = 1$, <1 , and >1 indicating neutral evolution, purifying selection, and positive selection respectively. Branch-site models were used that allowed ω to vary among the branches on the tree, testing whether a specific branch's ω was significantly different from that of the other branches. The branch-site Model A and the recommended test2 (a simplified version of model A with $\omega_2 = 1$) were therefore employed with each gene to test this hypothesis. The branch-site model A requires a-priori partitioning of the phylogeny into foreground and background branches and assumes that positive selection occurs along the foreground branch. The LRTs between nested models were conducted by comparing twice of the difference of the log-likelihood values ($2\Delta\ln L$) between two models. The significance of the LRT statistic was determined using a χ^2 distribution, with the standard degrees of freedom being used for each analysis. Potential positively selected sites (i.e. amino acid residues) were recorded according to high posterior probabilities following the Bayes empiri-

cal Bayes (BEB >0.95) prediction.

Evolutionary or parallel analysis

The maximal likelihood tree based on TSP-1 coding sequences of 24 species was used for evolutionary analysis. To infer convergent or parallel evolution sites of 24 species, ancestral sequences of TSP-1 were reconstructed by Ancestors program in the MEGA 7.0 software (42). The posterior probability of the reconstructed ancestral sites were used to evaluate the accuracy of the reconstruction results. In order to avoid the interference of the ancestral locus polymorphism in subsequent analysis, the site at which the posterior probability was less than 0.9 was abandoned. Then, the Jones-Taylor-Thornton (JTT) and Poisson amino acid substitution models (43) were used to test whether the probability of observed convergent or parallel sites were significantly higher than expected by chance.

Evaluation of the effects of mutation sites on the function of TSP-1

The effects of convergent or parallel evolution sites on the function of TSP-1 was predicted using ‘Sorting Tolerant From Intolerant’ (SIFT) algorithm (44). The TSP-1 sequence of *Mus musculus* (NP_035710.2) was used as a query sequence. Other parameters used default settings according to Kumar's studies.

Construction of space structure

The 3D structures of TSP-1 Subunit from *Myospalax baileyi* was modeled using the SWISS-MODEL (<https://swissmodel.expasy.org/>) (45) to assemble amino acids selected with a homology modeling protocol, and the 3D coordinates were constructed using Pymol software (46). Known homologues of TSP-1 were retrieved from the Protein Data Bank (PDB) (<http://www.pdb.org/>) and a PDB entry was identified to provide a suitable structural template. Based on the sequence alignment, the 3D structure of TSP-1 was constructed with a high level of confidence.

Determination of expression level of TSP-1 by Quantitative Real-time Polymerase Chain Reaction (qRT-PCR)

Total RNA was isolated from the liver, lung and skeletal muscle of *Myospalax baileyi* with Trizol reagent (Invitrogen Corp, USA). The RNA concentration and purity were assessed by ultraviolet (UV) spectrophotometry ($1.8 < A_{260}/A_{280} < 2.0$). The RNA integrity was checked via electrophoresis. Reverse transcription reaction was prepared with 3.8 μ g of total RNA using the First Strand cDNA Synthesis kit (Tiangen, China). To make standard curves, 1 μ L of first-strand cDNA was amplified with Premix Ex Taq Version Kit (TaKaRa Bio, Japan), and the quantified PCR products were used for plotting standard curves. The initial product concentration was set at 1 and standard curves were generated using a 10-fold serial dilutions ranging from 1 to 10^{-8} .

Quantitative real-time polymerase chain reaction (qRT-PCR) was performed using SYBR®Premix Ex Taq™ II (TaKaRa Bio, Japan) protocol on BIO-RAD Connect real-time PCR detection system with cycling conditions of 95°C for 3 min, followed by 40 cycles of 95°C for 30 sec and 60°C for 30 sec. β -Actin was used

as an internal control. The PCR primers for TSP-1 were: 5'-CGCTACAGGACAGCATTCGCAA-3'(sense); 5'-AGCCATCGTCAGCAGAGTCACT-3'(antisense). The amplicon length was 267 bp. The primer sequences for β -actin were: 5'-TCACCAACTGGGACGATATG-3'(sense); 5'-GTTGGCCTTAGGGTTCAGAG-3'(antisense); the amplicon length was 119bp. The TSP-1 mRNA level was normalized with β -actin mRNA to compensate for variations in initial RNA amounts. Normalization was carried out by dividing the logarithmic value of TSP-1 by the logarithmic value of β -actin (47).

Statistical analysis

Statistical analysis was performed with one-way analysis of variance (ANOVA) and Duncan's test using SPSS 17.0 (SPSS Inc., Chicago, IL, USA). A value of $p < 0.05$ was considered statistically significant.

Results

Sequence characterization of TSP-1

Complete TSP-1 coding sequences for 23 mammalian species were downloaded from 23 available published mammalian genome sequences from NCBI (www.ncbi.nlm.nih.gov):

Nannospalax galili (XM_017796147.1),
Rattus norvegicus (NM_001013062.1),
Mus musculus (BC050917.1),
Microtus ochrogaster (XM_005364238.2),
Mesocricetus auratus (XM_013122355.2),
Cricetulus griseus (XM_007628935.2),
Jaculus jaculus (XM_012949250.1),
Heterocephalus glaber (XM_004852682.3),
Fukomys damarensis (XM_015632040.2),
Cavia porcellus (XM_013158839.1),
Chinchilla lanigera (XM_013512591.1),
Octodon degus (XM_004623416.2),
Ictidomys tridecemlineatus (XM_013359376.2),
Ochotona princeps (XM_004578183.2),
Oryctolagus cuniculus (XM_002717799.3),
Bos grunniens (XM_014482984.1),
Bos taurus (NM_174196.1),
Ovis aries (XM_012131912.2),
Capra hircus (XM_018054475.1),
Homo sapiens (NM_003246.3),
Pan troglodytes (XM_016927922.1).

However, TSP-1 con-sequences of *Ochotona curzoniae* and *Ochotona collaris* were not found in NCBI.

In this study, TSP-1 subunit in *Myospalax baileyi*, *Nannospalax galili* and *Rattus norvegicus* were analyzed. The coding sequence (CDS) of *Myospalax baileyi* and *Nannospalax galili* TSP-1 subunits was 3516bp, and it encoded 1171 amino acids. The TSP-1 subunit of *Rattus norvegicus* studied was 3513 bp, and it encoded 1170 amino acids. Results of prediction of physicochemical properties showed that the TSP-1 subunit molecular weight of the three species were about 129KDa; the

theoretical isoelectric points (pI) in *Nannospalax galili* and *Rattus norvegicus* were lower than that in *Myospalax baileyi*. Isoelectric points are characteristic parameters of proteins and amino acids. While pI is not affected by external conditions such as pH and temperature, long-term evolutionary and environmental changes can cause mutations resulting in changes in amino acid sequence and changes in isoelectric point (Table 1).

Comparison of homologies

Results of homology analysis showed that the CDS of *Myospalaxbaileyi* TSP-1 nucleotide sequence had 95.08, 88.88, 90.76, 90.53, 90.81, 90.90, 90.70 and 89.9% homologies, while the amino acid sequence had 97.61, 93.08, 95.05, 95.13, 95.39, 95.22, 94.96 and 94.62% homologies with those of *Nannospalax galili*, *Heterocephalus glaber*, *Homo sapiens*, *Rattus norvegicus*, *Mus musculus*, *Cricetulus griseus*, *Mesocricetus auratus* and *Microtus ochrogaster*, respectively. From the phylogenetic tree, it was observed that plateau zokor had the highest homology with *Nannospalax galili*. These results are shown in Figure 1.

Construction of tree species from mtDNA data

To construct the phylogenetic tree, mtDNA sequences from 24 mammalian species (including 14 Rodentia, 4 Lagomorpha and 6 other mammalian species which served as Outgroup) were included in the study (Table 2). Bayesian phylogenetic reconstruction based on the nucleotide sequences yielded a tree with a topology similar to the well-accepted mammal species tree according to published phylogenetic studies. The mtDNA Bayesian tree which well supported the phylogeny of Rodentia, Lagomorpha and Outgroup and proved its accuracy was used as the input tree in this analysis [Bayesian posterior probability (BPP) = 100%] (Figure 2).

Selective pressure analysis

Selective pressure analysis reflects the fact that species are affected by their external environment. Site mutation may enhance the ability of species to adapt to

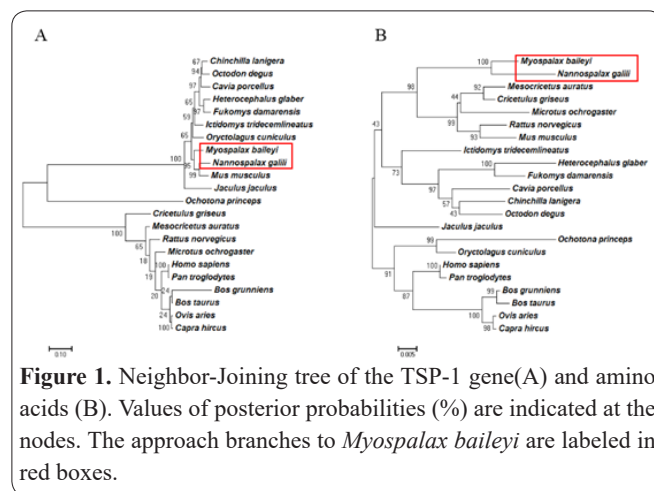


Figure 1. Neighbor-Joining tree of the TSP-1 gene (A) and amino acids (B). Values of posterior probabilities (%) are indicated at the nodes. The approach branches to *Myospalax baileyi* are labeled in red boxes.

Table 1. Physicochemical properties of anti-angiogenesis protein TSP-1 subunit.

| Protein | Species | Number of amino acids | Molecular weight | Theoretical pI |
|---------|---------------------------|-----------------------|------------------|----------------|
| TSP-1 | <i>Myospalax baileyi</i> | 1171 | 129606.24 | 4.79 |
| | <i>Nannospalax galili</i> | 1171 | 129818.01 | 4.76 |
| | <i>Rattus norvegicus</i> | 1170 | 129671.26 | 4.74 |

Table 2. Names of 24 kinds of mammals with placenta and their IDs in GenBank.

| Class | Species | Common name | GenBank ID |
|------------|-----------------------------------|--|-------------|
| Rodentia | <i>Mospalax baileyi</i> | Plateau zokor | NC_018098.1 |
| | <i>Nannospalax galili</i> | Northern Israeli blind subterranean mole rat | JN571132.1 |
| | <i>Rattus norvegicus</i> | Rat | KF011917.1 |
| | <i>Mus musculus</i> | Mouse | J01420.1 |
| | <i>Microtus ochrogaster</i> | Prairie vole | NC_027945.1 |
| | <i>Mesocricetus auratus</i> | Golden hamster | EU660218.1 |
| | <i>Cricetulus griseus</i> | Chinese hamster | DQ390542.2 |
| | <i>Jaculus jaculus</i> | African jerboa | NC_005314.1 |
| | <i>Heterocephalus glaber</i> | African Naked Mole-Rat | HQ689652.1 |
| | <i>Fukomys damarensis</i> | Damara Mole Rat | KT321364.1 |
| | <i>Cavia porcellus</i> | Guinea pig | NC_000884.1 |
| | <i>Chinchilla lanigera</i> | Chinchilla | NC_021386.1 |
| | <i>Octodon degus</i> | Degu | HM544134.1 |
| | <i>Ictidomys tridecemlineatus</i> | Thirteen-linedground squirrels | NC_027278.1 |
| Lagomorpha | <i>Ochotona curzoniae</i> | Plateau pika | EF535828.1 |
| | <i>Ochotona princeps</i> | American pika | NC_005358.1 |
| | <i>Ochotona collaris</i> | Collared pika | AF348080.1 |
| | <i>Oryctolagus cuniculus</i> | Rabbit | NC_001913.1 |
| Outgroup | <i>Bos grunniens</i> | Yak | AY684273.2 |
| | <i>Bos Taurus</i> | Cow | V00654.1 |
| | <i>Ovis aries</i> | Sheep | KR868678.1 |
| | <i>Capra hircus</i> | Goat | KY305183.1 |
| | <i>Homo sapiens</i> | Human | V00662.1 |
| | <i>Pan troglodytes</i> | Chimpanzee | NC_001643.1 |

the hypoxic environment effectively. To detect the positively selected sites of TSP-1 in plateau zokor, the plateau zokor branch was treated as the foreground branch. Using the LRT test based on the branch-site model for TSP-1 gene, it was observed that there were no positive selection sites in plateau zokor TSP-1 ($P > 0.05$) (Table 3).

Evolutionary analysis

Although no statistically significant positively selected sites were detected in the TSP-1 in plateau zokor, it did not indicate that the TSP-1 did not adaptively evolve in these species. Convergent or parallel evolution is a strong evidence for adaptive evolution. To detect the convergent sites in subterranean rodents in response to hypoxia environments, convergent changes were identified by comparing ancestral and extended TSP-1 protein sequences. It was observed that eight sites experienced parallel evolution on subterranean rodent branch of *Eospalax baileyi* and *Nannospalax galili*. The 19th, 65th, 185th, 270th, 517th, 536th, 1052th and 1092th positions of TSP-1 were asparagine (N, Asn), asparagine (N, Asn), serine (S, Ser), isoleucine (I, Ile), serine (S, Ser), valine (V, Val), asparagine (N, Asn) and arginine (R, Arg),

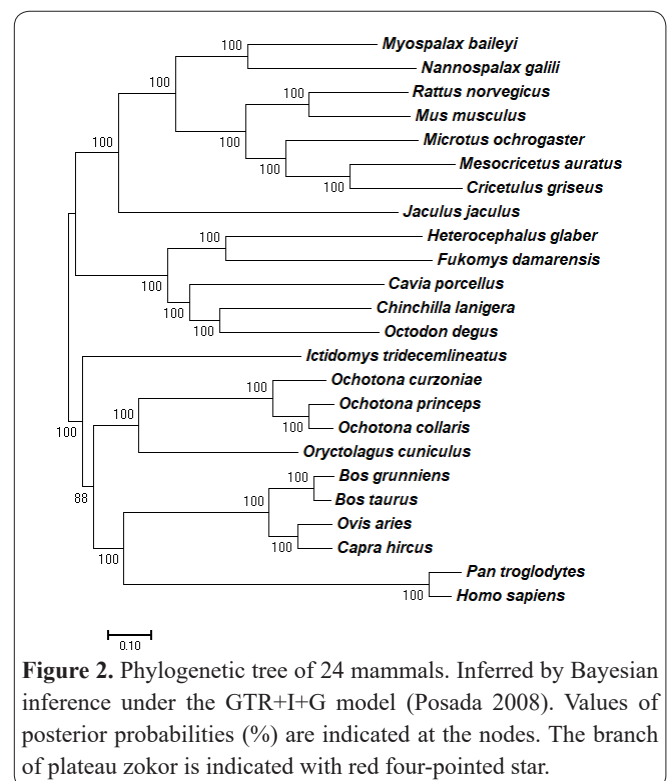


Figure 2. Phylogenetic tree of 24 mammals. Inferred by Bayesian inference under the GTR+I+G model (Posada 2008). Values of posterior probabilities (%) are indicated at the nodes. The branch of plateau zokor is indicated with red four-pointed star.

Table 3. Likelihood values, parameter estimates and sites under positive selection for TSP-1 in plateau zokor.

| Genes | Model code | Estimate of parameters | -lnL ^a | Model comparison | Positively selected sites | 2ΔlnL (p-value) |
|-------|---------------------|---|-------------------|--------------------|---------------------------|-------------------|
| TSP-1 | Branch-site e Model | | | | | |
| | Null A | p0=0.947, p1=0.053, (p2+p3=0), ω0=0.030, ω1=1, ω2=1 | 16199.13 | | NA | |
| | Model A | p0=0.947, p1=0.053, (p2+p3=0), ω0=0.030, ω1=1, ω2=1 | 16199.13 | Model A vs. Null A | Not Found | 0 ($p = 1.000$) |

^alnL is the log-likelihood score. * $P > 0.95$, ** $P > 0.99$.

respectively on the ancestral branch. The same replacements of serine (S, Ser), serine (S, Ser), aspartic acid (D, Asp), threonine (T, Thr), asparagine (N, Asn), glutamic acid (E, Glu), lysine (K, Lys) and threonine (T, Thr) occurred on subterranean rodent branch of *Eospalax baileyi* and *Nannospalax galili*. Statistical test (34) showed that the eight parallel evolution sites were significantly greater than random expectations ($p < 0.01$), suggesting selection rather than chance (Figure 3).

Evaluation of the effects of the convergent evolution sites on the function of TSP-1

According to the SIFT algorithm, if the score is less than 0.05, the amino acid mutation has an effect on the function of the protein, and vice versa. The results revealed that the convergent evolution sites (Asp185, Thr270, Glu536 and Thr1092) showed significant effects on the function of TSP-1. Otherwise, the convergent evolution site (Ser19, Ser65, Asn517 and Lys1052) showed no significant effects on the function of TSP-1 (Table 4).

Construction of TSP-1 3D structure

A template structure was selected from Protein data bank (PDB) (Model A: 1az4 was from amino acids 29 to 233, Model B: 3r6b was from amino acids 435 to 548, Model C: 1ux6 was from amino acids 834 to 1170) to simulate the 3D structure of TSP-1. Thrombospondin-1 (TSP-1) is a homologous trimer consisting of three identical peptide chains. Each polypeptide chain consists of the NH₂-terminal, the procollagen homology domain (PC), type I repeats, type II repeats, type III repeats, and the COOH-terminal six functional regions. The type I repeats are composed of three thrombospondin type 1 repeats (TSRs), i.e. TSR1, TSR2 and TSR3; and there is a specific amino acid sequence CSVTCG in TSR2 and TSR3 motif, which is specifically combined with CD36 receptor. The peptide 4N1K of C-Terminal combines with CD47 receptor (integrin-associated protein). From the 3D models, it was found that mutation site 185 Asp was located in the NH₂-terminal of TSP-1 in Model A. However, Thr270 was located in the NH₂-terminal but it was not built in Model A, because the Model A structure from PDB was not complete NH₂ terminal of TSP-1, this region is usually combined with low density lipoprotein receptor-like protein (LRP1) to inhibit activation of matrix metalloprotease (MMP), and reduce the expression of VEGF, which regulates the activity of the protease and mediates the combination of TSP-1 with heparin sulfate polysaccharide and integrin-associated protein. This results in inhibition of the adhesion between endothelial cells and matrix fibronectin, and indirectly restrains the proliferation and angiogenesis of endothelial cells. The Type I repeats existed in mutation sites Glu536, type I repeat domain is composed of three groups of repetitive peptide sequences (TSR1, TSR2 and TSR3). The sequence of CSVTCG in TSR2 and TSR3 (amino acids 448-510) is specifically associated with CD36. Nonpolar amino acids are hydrophobic and more likely to bind to CD36 on the surface of endothelial cells, thus activating Fyn (non-receptor protein tyrosine kinase) to further activate the downstream p38 mitogen-induced apoptosis of endothelial cells, thereby inhibiting angiogenesis. Thr1092 located in COOH terminal that consists of a hydrophobic group 4N1K,

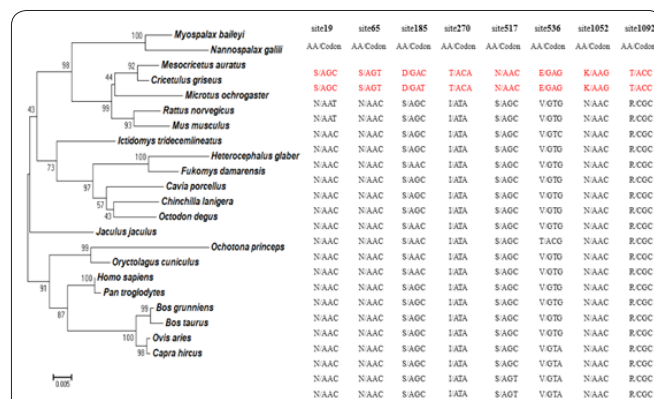


Figure 3. Convergent evolution sites of the TSP-1 sequence. Amino acids and codons of eight sites are shown. *Eospalax baileyi* and *Nannospalax galili* are highlighted with red color, while the other species are shown in black color.

Table 4. The effects of convergent evolution sites on the function of TSP-1.

| Protein | Substitution | SIFT score | SIFT Prediction (cutoff=0.05) |
|---------|--------------|------------|-------------------------------|
| TSP-1 | S185D | 0.017 | Damaging |
| | I270T | 0.003 | Damaging |
| | V536E | -0.379 | Damaging |
| | R1092T | 0.050 | Damaging |
| | N19S | 0.585 | Tolerated |
| | N65S | 0.064 | Tolerated |
| | S517N | 0.174 | Tolerated |
| | N1052K | 0.796 | Tolerated |

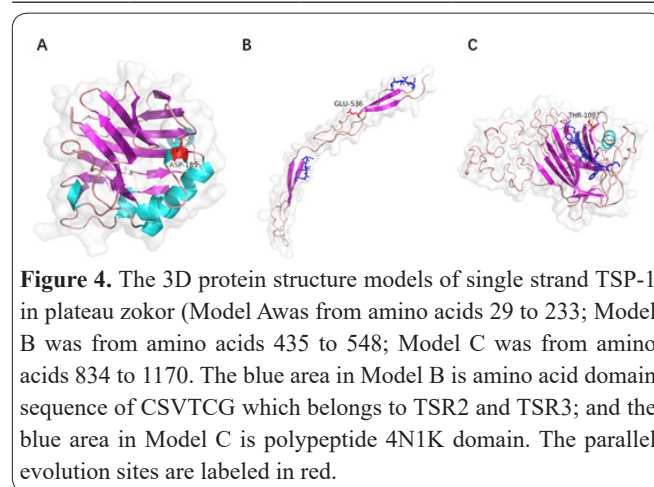


Figure 4. The 3D protein structure models of single strand TSP-1 in plateau zokor (Model A was from amino acids 29 to 233; Model B was from amino acids 435 to 548; Model C was from amino acids 834 to 1170). The blue area in Model B is amino acid domain sequence of CSVTCG which belongs to TSR2 and TSR3; and the blue area in Model C is polypeptide 4N1K domain. The parallel evolution sites are labeled in red.

which binds to the integrin-related protein CD47 (integrin-associated protein, IAP), mediates cell adhesion and platelet aggregation, and inhibits the proliferation of endothelial cells. Different functional regions of TSP-1 work with different anti-angiogenesis mechanisms, and mutation sites may have a great influence on function of TSP-1 (Figure 4).

qRT-PCR Assay of TSP-1 mRNA expression

The mRNA expression levels of TSP-1 in plateau zokor and SD rat at altitudes of 3 300 m and 2 260 m were determined in the liver, lung and skeletal muscle using qRT-PCR analysis (Table 5).

For all tissues, the expression levels of TSP-1 in plateau zokor were significantly higher in the 3 300 m group than in the 2 260 m group ($p < 0.01$). However, there was no difference between the 3 300 m and 2 260 m groups of SD rats in the three tissues. The relative

Table 5. Quantification mRNA levels of TSP-1 at altitudes of 3 300 m and 2 260 m.

| Tissue | Plateau zokor | | SD rat | |
|-----------------|-----------------|---------------|---------------|---------------|
| | 3 300 m | 2 260 m | 3 300 m | 2 260 m |
| Liver | 0.193 ± 0.007** | 0.042 ± 0.006 | 0.006 ± 0.001 | 0.009 ± 0.003 |
| Lung | 0.088 ± 0.013** | 0.028 ± 0.008 | 0.007 ± 0.001 | 0.002 ± 0.001 |
| Skeletal muscle | 0.089 ± 0.003** | 0.029 ± 0.002 | 0.006 ± 0.002 | 0.008 ± 0.002 |

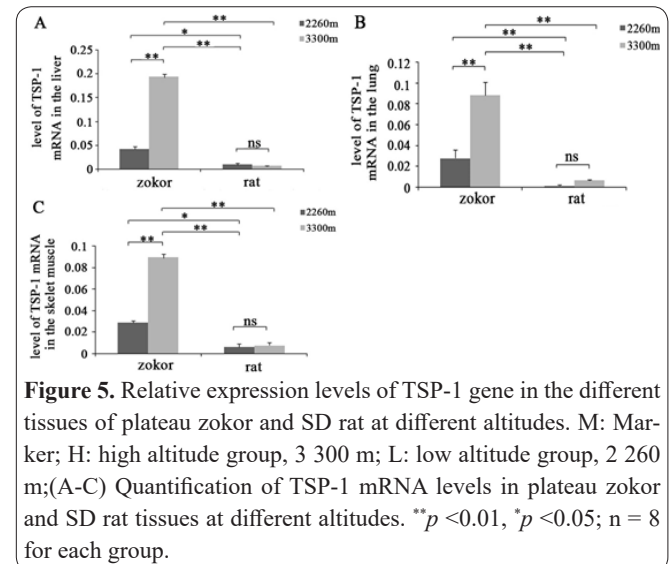
** $p < 0.01$, * $p < 0.05$; n = 8 for each group.

expression levels of TSP-1 in plateau zokor in the three tissues were significantly higher than those in SD rat in the 3 300 m and 2 260 m groups ($p < 0.05$). These results are shown in Figure 5.

Discussion

The plateau zokor belongs to the order Rodentia, in the Cricetidae family, and genus *Myospalax* (48). From the phylogenetic homology tree, it was observed that plateau zokor shared high homology with *Nannospalax galili*. The two species are far apart in classification, but their lifestyles and morphologies are similar. They spend their whole lives in underground sealed burrows, in extreme hypoxia and hypercapnia especially during the rainfall and flood periods (22, 49). These species are grouped into a large branch with *R. norvegicus*. *Heterocephalus glaber* belongs to the family of subterranean rodents. However, this species was far removed from other subterranean rodents. Studies on the phylogenetic relationship based on genome and transcriptome analysis have found that the plateau zokor diverged from the rat approximately 52 million years ago (50).

Thrombospondin-1 (TSP-1) is released from multiple cells including platelets, endothelial cells, keratinocytes and fibroblasts (51). The coding sequence (CDS) of *Myospalax baileyi* and *Nannospalax galili* TSP-1 subunit was 3516 bp, encoding 1171 amino acids. The theoretical pI values of the protein in *Nannospalax galili* and *Rattus norvegicus* were lower than that in *Myospalax baileyi*, indicating that physicochemical properties of genes are changed by the living environment. This affects functions such as targeting cells for apoptosis, clearance of apoptotic cells by macrophages and regulation of vascular endothelial cell formation by binding to a variety of function domains to extracellular matrix proteins (52). Previous TSP-1 studies revealed that asparagine(N) mutated to aspartic acid(D) at position 362 of TSP-1 in familial pulmonary hypertension, which induced less than half of the ability of TSP-1 to activate TGF- β binding to CD36, and increased proliferation of endothelial cells and smooth muscle cells (10). Genome and transcriptome data have shown that TSP-1 is not positively selected in subterranean rodents (28, 53). In the present study, the LRT test based on the branch-site model A for TSP-1 gene indicated there were no positive selection sites in plateau zokor ($P > 0.05$). This suggests that variation in ω -ratios across the phylogeny are not attributed to positive selection in the TSP-1 of the foreground branch. This is in agreement with previous studies which reported that its upstream target gene *p53* was not positively selected in plateau zokor (53, 54). Compared to other species with respect to the amino acid sequence of TSP-1 protein, it was observed that there were eight common parallel evolu-



tion sites in *Eospalax baileyi* and *Nannospalax galili*, which were located in the functional regions. Using SIFT algorithm, it was shown that the parallel evolution sites (Asp185, Thr270, Glu536 and Thr1092) exerted significant effects on the function of TSP-1 in plateau zokor. The 3D structure constructed revealed these four parallel evolutionary sites in different functional areas. Firstly, there were two common mutation sites Asp185 and Thr270NH₂-terminal domain. In contrast, in Ser185 and Ile270 in SD rat, there were switches between polar and nonpolar amino acids. Changes in polarity and electric charge may enhance the affinity of binding to LRP1 (55-58). Secondly, a mutation site Glu536 located near CSVTG domain may affect their interaction with the amino acids around them. Compared with Val536 in SD rat, there was a switch from nonpolar amino acid to negative electrode polar amino acid (59). Thirdly, the COOH-terminal domain mutation site Thr1092, in contrast, Arg1092 in SD rat, there was a switch from positive electrode polar amino acid to nonpolar amino acid (60). It is predicted that these evolution sites may play significant roles in extreme environmental adaptation of plateau zokor, but further investigations are needed to confirm this.

In this study, it was shown that the expression level of TSP-1 was related to degree of hypoxia. Under normal condition, TSP-1 is expressed at low levels in most cells. In contrast, its expression level increases and stabilizes in response to unrestricted increase in microvessel density in hypoxia, so as to maintain dynamic balance with VEGF, thus maintaining the stability of internal environment of angiogenesis (11,13,14). With aggravation of hypoxia, there is a breakdown in the balance of angiogenesis in tumor cells, and the ratio of TSP-1/VEGF gradually decreases and microvessel density increases, thereby accelerating angiogenesis of tumor tissues. However, after over expression of TSP-

1, the vascular density in tumor cells decreases significantly, and the blood supply decreases, resulting in the necrosis of tumor cells. Thus, TSP-1 is an effective inhibitor of angiogenesis. In the present study, it was found that the expression level of TSP-1 in the tissues of liver, lung and skeletal muscle of plateau zokor were increased significantly from 2260m to 3300m, but there was no corresponding significant difference in TSP-1 expression in SD rat under the same conditions. Thus, TSP-1 gene is expressed in different patterns in the two species (61, 62). It is known that TSP-1 is the first endogenous angiogenesis inhibitor identified in *p53* pathway (63-68). The *p53* gene can positively stimulate the TSP-1 promoter sequence (+516 -+538), and inhibit angiogenesis by up-regulating the expression of TSP-1 (70-71). The *P53* of plateau zokor is sensitive to environmental oxygen concentration; its expression level at 2260 m was 80% lower than that at 3300 m (54). The different expression patterns in the two species could be due to differences in the regulations of upstream genes and downstream target genes.

In conclusion, due to long time adaption to the hypoxic environment of sealed burrows, plateau zokor upregulates the expression of TSP-1 for anti-angiogenesis. The mutation sites found in TSP-1 of plateau zokor may play important roles in inhibiting angiogenesis.

Acknowledgments

This work was supported by the Natural Science Foundation of Qinghai Province (No.2016-ZJ-901).

Conflict of Interest

The authors declare no conflict of interest.

Author's contribution

All work was done by the authors named in this article and the authors accept all liability resulting from claims relating to this manuscript and its contents. The study was conceived and designed by Dengbang Wei. Suhua Li, Bo Xu, Zhifang An, Zhijie Wang, Yongxiao Li, Lian Wei, Dengbang Wei collected and analysed the data. Suhua Li wrote the manuscript. All authors have read and approved the text prior to publication.

References

- Heidenreich R, Rocken M, Ghoreschi K. Angiogenesis drives psoriasis pathogenesis. *Int J Exp Pathol* 2009; 90:232-248.
- Shweiki D, Itin A, Soffer D, Keshet E. Vascular endothelial growth factor induced by hypoxia may mediate hypoxia-initiated angiogenesis. *Nat* 1992; 359: 843-845.
- Forsythe JA, Jiang BH, Iyer NV, Agani F, Leung SW, Koos RD, et al. Activation of vascular endothelial growth factor gene transcription by hypoxia-inducible factor 1. *Mol Cell Biol* 1996; 16: 4604-4613.
- Ravi R, Mookerjee B, Bhujwala ZM, Sutter CH, Artemov D, Zeng Q, et al. Regulation of tumor angiogenesis by p53-induced degradation of hypoxia-inducible factor 1alpha. *Genes Dev* 2000; 14:34-44.
- Liao D, Johnson RS. Hypoxia: A key regulator of angiogenesis in cancer. *Cancer Metastasis Rev* 2007; 26: 281-290.
- Teodoro JG, Evans SK, Green MR. Inhibition of tumor angiogenesis by p53: a new role for the guardian of the genome. *J Mol Med* 2007; 85: 1175-1186.
- Paul B. Thrombospondins function as regulators of angiogenesis. *J Cell Commun Signal* 2009; 3:189-200.
- Silverstein RL. The face of TSR revealed: an extracellular signaling domain is exposed. *J Cell Biol* 2002; 159: 203-206.
- Bornstein P. Thrombospondins function as regulators of angiogenesis. *J Cell Commun Signal* 2009; 3:189-200.
- Maloney JP, Stearman RS, Bull TM, Calabrese DW, Tripp-Addison ML, Wick MJ, et al. Loss-of-function thrombospondin-1 mutations in familial pulmonary hypertension. *Am J Physiol Lung Cell Mol Physiol* 2012; 302: 541-554.
- Phelan MW, Forman LW, Perrine SP, Faller DV. Hypoxia increases thrombospondin-1 transcript and protein in cultured endothelial cells. *J Lab Clin Med* 1998; 132:519-529.
- Fontana A, Fileur S, Guglielmi J, Frappart L, Bruno-Bossio G, Boissier S, et al. Human breast tumors override the antiangiogenic effect of stromal thrombospondin-1 in vivo. *Int J Cancer* 2005; 116:686-691.
- Takahashi M, Oka M, Ikeda T, Akiba S, Sato T. Role of thrombospondin-1 in hypoxia-induced migration of human vascular smooth muscle cells. *Yakugaku Zasshi J Pharm* 2008; 128:377-383.
- Morgan RL, Nikitorowicz J, Shiwen X, Leask A, Tsui J, Abraham D, et al. Thrombospondin 1 in hypoxia-conditioned media blocks the growth of human microvascular endothelial cells and is increased in systemic sclerosis tissues. *Fibrogenesis Tissue Repair* 2011; 4: 13.
- Fan NC, Shi YZ. Taxonomy of Chinese zokor (*Eospalax*) subgenus. *Acta Theriologica Sinica* 1982; 2: 183-199.
- Wilson DE, Reeder DM. *Mammal Species of the World: A Taxonomic and Geographic Reference* (3rd Ed), Johns Hopkins University Press, 2005.
- Nevo E, Ivanitskaya E, Beiles A. Adaptive radiation of blind subterranean mole rats: naming and revisiting the four sibling species of the *Spalax ehrenbergi* superspecies in Israel: *Spalax galili* (2n=52), *S. golani* (2n=54), *S. carmeli* (2n=58), and *S. judaei* (2n=60). *Balkhuys Publishers, Leiden*. 2001.
- Shams I, Avivi A, Nevo E. Oxygen and carbon dioxide fluctuations in burrows of subterranean blind mole rats indicate tolerance to hypoxic-hypercapnic stresses. *Comp Biochem Physiol A* 2005; 142:376-382.
- Wei DB, Wei L, Zhang JM, Yu HY. Blood-gas properties of plateau zokor (*Myospalaxbaileyi*). *Comp Biochem Physiol* 2006; 145: 372-375.
- Zheng YN, Zhu RJ, Wang DW, Wei L, Wei DB. Gene coding and mRNA expression of vascular endothelial growth factor as well as microvessel density in brain of plateau zokor: comparison with other rodents. *Acta Physiologica Sinica* 2011; 63: 155-163.
- Vleck D. Burrow structure and foraging costs in the fossorial rodent, *Thomomys bottae*. *Oecologia* 1981; 49: 391-396.
- Nevo E. Mosaic evolution of subterranean mammals: regression, progression and global convergence. *Oxford University Press, Oxford*. 1999.
- Gurnett AM, O'Connell JP, Harris DE, Lehmann H, Joysey KA, Nevo E. The myoglobin of rodents: *Lagostomus maximus* (viscacha) and *Spalax ehrenbergi* (mole rat). *J Prot Chem* 1984; 3: 445-454.
- Kleinschmidt T, Nevo E, Goodman M, Braunitzer G. Mole rat hemoglobin: primary structure and evolutionary aspects in a second karyotype of *Spalax ehrenbergi*, Rodentia, (2n=52). *Biol Chem Hoppe Seyler* 1985; 366: 679-685.
- Widmer HR, Hoppeler H, Nevo E, Richard TC, Weibel ER. Working underground: Respiratory adaptations in the blind mole rat. *Proc Natl Acad Sci USA* 1997; 94: 2062-2067.
- Howell K, Ooi H, Preston R, McLoughlin P. Structural basis of hypoxic pulmonary hypertension: the modifying effect of chronic hypercapnia. *Exp Physiol* 2004; 89:66-72.

27. Yang ZY, Zhang Y, Chen LN. Single amino acid changes in naked mole rat may reveal new anti-cancer mechanisms in mammals. *Gene* 2015; 572: 101-107.
28. Kim EB, Fang X, Fushan AA, Huang Z, Lobanov AV, Han L, Marino SM, Sun X, Turanov AA, Yang P, Yim SH, Zhao X, Kasai-kina MV, Stoletzki N, Peng C, Polak P, Xiong Z, Kiezun A, Zhu Y, Chen Y, Kryukov GV, Zhang Q, Peshkin L, Yang L, Bronson RT, Buffenstein R, Wang B, Han C, Li Q, Chen L, Zhao W, Sunyaev SR, Park TJ, Zhang G, Wang J, Gladyshev VN. Genome sequencing reveals insights into physiology and longevity of the naked mole rat. *Nature* 2011; 479, 223-227.
29. Wei DB, Wei L. The Mensuration Results of the Number of Red Cell, the Density of Hemoglobin and the Contents of Myoglobin in Plateau Zokor. *J Qinghai Univ* 2001; 19: 1-2.
30. Avivi A, Resnick MB, Nevo E, Joel A, Levy AP. Adaptive hypoxic tolerance in subterranean mole rat *Spalax ehrenbergi*: the role of vascular endothelial growth factor. *FEBS Lett* 1999; 452: 133-140.
31. Burland TG. DNASTAR's Lasergene sequence analysis software. *Methods Mol Biol* 2000; 132:71-91.
32. Kumar S, Stecher G, Tamura K. MEGA7: Molecular evolutionary genetics analysis version 7.0 for bigger datasets. *Mol Biol Evol* 2016; 33:1870-1874.
33. Huelsenbeck JP, Ronquist F. MRBAYES: Bayesian inference of phylogenetic trees. *Bioinform* 2001; 17:754-755.
34. Gamerman D, Lopes HF. Markov chain Monte Carlo: stochastic simulation for Bayesian inference. Boca Raton: CRC Press. 2006.
35. Darriba D, Taboada GL, Doallo R, Posada D. jModelTest 2: more models, new heuristics and parallel computing. *Nat Methods* 2012; 9:772-772.
36. Yamaoka K, Nakagawa T, Uno T. Application of Akaike's information criterion (AIC) in the evaluation of linear pharmacokinetic equations. *J Pharmacokinet Biopharm* 1978; 6:165-175.
37. Sakamoto Y, Ishiguro M, Kitagawa G. Akaike information criterion statistics. Dordrecht, The Netherlands: D. Reidel, 81.1986.
38. Bozdogan H. Model selection and Akaike's information criterion (AIC): The general theory and its analytical extensions. *Psychometrika* 1987; 52:345-370.
39. Yang Z. PAML 4: phylogenetic analysis by maximum likelihood. *Mol Biol Evol* 2007; 24:1586-1591.
40. Zhang J, Nielsen R, Yang Z. Evaluation of an improved branch-site likelihood method for detecting positive selection at the molecular level. *Mol Biol Evol* 2005; 22: 2472-2479.
41. Wang Z, Xu S, Du K, Huang F, Chen Z, Zhou K, et al. Evolution of digestive enzymes and RNASE1 provides insights into dietary switch of cetaceans. *Mol Biol Evol* 2016; 33: 3144-3157.
42. Nei M, Kumar S. Molecular evolution and phylogenetics. Oxford university press. 2000.
43. Zhang J, Kumar S. Detection of convergent and parallel evolution at the amino acid sequence level. *Mol Biol Evol* 1997; 14:527-536.
44. Kumar P, Henikoff S, Ng PC. Predicting the effects of coding non-synonymous variants on protein function using the sift algorithm. *Nat Protoc* 2009; 4: 1073-1081.
45. Arnold K, Bordoli L, Kopp J, Schwede T. The SWISS-MODEL workspace: a web-based environment for protein structure homology modelling. *Bioinformatics* 2006;22: 195-201.
46. Schrodinger LLC. The PYMOL molecular graphics system, Version 1.4.1. 2010.
47. Niesters HG. Quantitation of viral load using real-time amplification techniques. *Methods* 2001; 25: 419-429.
48. Zeng J, Wang Z, Shi Z. Metabolic characteristics and some physiological parameters of the mole rat (*Myospalaxbaileyi*) in an alpine area. *Acta Biol Plat Sin* 1984; 3:163-171.
49. Wei DB, Wang DW, Wei L, Ma BY. Differences in Physiological Adaptive Strategies to Hypoxic Environments in Plateau Zokor and Plateau Pika. *High Alt Med* 2012; 36: 1.
50. Shao Y, Li JX, Ge RL, Zhong L, Irwin DM, Murphy RW, et al. Genetic adaptations of the plateau zokor in high-elevation burrows. *Sci Rep UK* 2015; 5: 17262.
51. Kazerounian S, Yee KO, Lawler J. Thrombospondins in cancer. *Cell Mol Life Sci* 2008; 65: 700-712.
52. Clezardin P, Frappart L, Clerget M, Pechoux C, Delmas PD. Expression of thrombospondin (TSP1) and its receptors (CD36 and CD51) in normal, hyperplastic, and neoplastic human breast. *Cancer Res* 1993; 53:1421-1430.
53. Fang X, Nevo E, Han L, Levanon EY, Zhao J, Avivi A, Larkin D, Jiang X, Feranchuk S, Zhu Y, Fishman A, Feng Y, Sher N, Xiong Z, Hankeln T, Huang Z, Gorbunova V, Zhang L, Zhao W, Wildman DE, Xiong Y, Gudkov A, Zheng Q, Rechavi G, Liu S, Bazak L, Chen J, Knisbacher BA, Lu Y, Shams I, Gajda K, Farre M, Kim J, Lewin HA, Ma J, Band M, Bicker A, Kranz A, Mattheus T, Schmidt H, Seluanov A, Azpurua J, McGowen MR, Jacob EB, Li K, Peng S, Zhu, X, Liao X, Li S, Krogh A, Zhou X, Brodsky L, Wang J. Genome-wide adaptive complexes to underground stresses in blind mole rats *Spalax*. *Nat Commun* 2014, 5, 3966. DOI:10.1038/ncomms4966.
54. Zhao Y, Ren JL, Wang MY, Zhang ST, Liu Y, Li M, et al. Codon 104 variation of p53 gene provides adaptive apoptotic response to extreme environments in mammals of the Tibet plateau. *P Natl Acad Sci USA* 2013; 110: 20639-20644.
55. An ZF, Zhao K, Wei LN, Wang ZJ, Li SH, Wei L, et al. p53 gene cloning and response to hypoxia in the plateau zokor, *Myospalaxbaileyi*. *Animal Biol* 2018; 12: 3.
56. Chen H, Sottile J, Strickland DK, Mosher DF. Binding and degradation of thrombospondin-1 mediated through heparansulphate proteoglycans and low-density-lipoprotein receptor-related protein: localization of the functional activity to the trimeric N-terminal heparin-binding region of thrombospondin-1. *Biochem J* 1996; 318: 959-963.
57. Yang Z, Strickland DK, Bornstein P. Extracellular matrix metalloproteinase 2 levels are regulated by the low density lipoprotein related scavenger receptor and thrombospondin 2. *J Biol Chem* 2001; 276:8403-8408.
58. Hahn-Dantona E, Ruiz JF, Bornstein P, Strickland DK. The low density lipoprotein receptor-related protein modulates levels of matrix metalloproteinase 9 (MMP-9) by mediating its cellular catabolism. *J Biol Chem* 2001; 276:15498-15503.
59. Greenaway J, Moorehead RP, Bornstein P, Lawler J, LaMarre J, Petrik J. Thrombospondin-1 inhibits VEGF levels in the ovary directly by binding and internalization via the low density lipoprotein receptor-related protein-1 (LRP-1). *J Cell Physiol* 2007; 210:807-818.
60. Febbraio M, Hajjar DP, Silverstein RL. CD36: a class B scavenger receptor involved in angiogenesis, atherosclerosis, inflammation and lipid metabolism. *J Clin Invest* 2001; 108:785-791.
61. Yasuyoshi M, Shin-ichi W, Hiroshi K, Hideki S. Thrombospondin-1-derived 4N1K peptide expression is negatively associated with malignant aggressiveness and prognosis in urothelial carcinoma of the upper urinary tract. *BMC Cancer* 2012; 12: 2-9.
62. Goldshmidt O, Zcharia E, Abramovitch R, Metzger S, Aingorn H, Friedmann Y, et al. Cell surface expression and secretion of heparanase markedly promote tumor angiogenesis and metastasis. *Proc Natl Acad Sci USA* 2002; 99: 10031-10036.
63. Luke MR, Joanna N, Xu SW, Andrew L, Janice T, David A, et al. Thrombospondin 1 in hypoxia-conditioned media blocks the growth of human microvascular endothelial cells and is increased in systemic sclerosis tissues. *Fibrogenesis Tissue Repair* 2011; 4:13.
64. Good DJ, Polverini PJ, Rastinejad F, Le Beau MM, Lemons

RS, Frazier WA, et al. A tumor suppressor-dependent inhibitor of angiogenesis is immunologically and functionally indistinguishable from a fragment of thrombospondin. *Proc Natl Acad Sci USA* 1990; 87: 6624-6662.

65. Dameron KM, Volpert OV, Tainsky MA, Bouck N. Control of angiogenesis in fibroblasts by p53 regulation of thrombospondin-1. *Sci* 1994; 21:1582-1584.

66. Mutalifu Z, Buranjiang G, Jin H. Activating transcription factor 3 enhances chemosensitivity of dichloroacetic acid via p53 pathway in cervical squamous epithelial cancer cells. *Trop J Pharm Res* 2018; 17(12): 2393-2398.

67. Qin WY, Zhong JR, Rong XF, Zhong Y. Protective effects of Zhweifeng tougu on collagen-induced arthritis in DBA/1 mice. *Trop J*

Pharm Res 2018; 17(12): 2439-2444.

68. Wang H, Qiao W. Curcumin induces apoptosis in lung cancer cells via mitochondria-dependent signal pathways. *Trop J Pharm Res* 2018; 17(10): 1933-1938.

69. Ni H, Hao RL, Li XF, Raikos V, Li HH. Synergistic anticancer and antibacterial activities of cordycepin and selected natural bioactive compounds. *Trop J Pharm Res* 2018; 17(8): 1621-1627.

70. Lawler J, Miao W M, Duquette M. Thrombospondin-1 gene expression affects survival and tumor spectrum of p53-deficient mice. *Am J Pathol* 2001; 159: 1949-1956.

71. Wang MY, Zhao Y, Zhang ST, Chen XQ, Du JZ. The regulation of expression for p53 and its target genes in simulate hypoxia. *China J ApplPhysiol* 2013; 29: 136-138.